Electronic Band Structure of Selenium and Tellurium

JOHN R. REITZ*
National Carbon Research Laboratories,† Parma, Ohio
(Received November 15, 1956)

The band structure of selenium and tellurium has been calculated according to the tight-binding scheme in which only nearest neighbor interactions are presumed to be important. As a first approximation, von Hippel's hypothetical crystal with 90° bond angles between bonds in the chain is used, and the ninth degree secular equation for the p bands factors into three identical cubic equations. Next, the crystal is pulled out along the c axis to the observed bond angle, and further splitting of the p bands is calculated as a perturbation. The fifteen d bands are also computed, and mixing of p and d levels estimated. In addition, matrix elements for optical transitions between bands have been worked out. The long-wavelength absorption limit for direct transitions occurs at $k_z=\pi/c$, and is different for light polarized parallel or perpendicular to the c axis of the crystal. Both $p\rightarrow p$ and $p\rightarrow d$ transitions give the same order for the two absorption edges, the results appearing to be in accord with experiments of Loferski on tellurium. Finally, we note Bridgman's measurements on crystals of tellurium subjected to hydrostatic pressure: the bond angle apparently *increases* with pressure. The calculations here show a reduction in energy gap with increasing bond angle (i.e., increasing pressure), which is in the right direction to explain the simultaneous large decrease in electrical resistivity observed by Bridgman

I. INTRODUCTION

SELENIUM and tellurium share an unusual hexagonal crystal structure, space group D_3^4, the atoms being arranged in spiral chains which are oriented along the c axis of the crystal. The hexagonal lattice is achieved by locating a chain at the center and at each of the six corners of a hexagon. There are three atoms per primitive unit cell. Figure 1 shows a view of this structure in the direction of the c axis. Each atom forms covalent bonds with the two nearest neighbors in its chain, the bond angle being close to 90° (Se: 105.5°; Te: 102.6°). The various chains are rather weakly held together; in the nearest neighbor approximation the chains are, of course, completely independent of each other. In both selenium and tellurium, however, the four second neighbors of an atom are on adjacent chains. A detailed discussion of the selenium structure, together with its relation to other group VIb structures, has been given by von Hippel.[1]

Although selenium is one of the older semiconductors and of some commercial importance, very little is known about its electronic structure. The cohesion of the spiral chain is usually explained from the Heitler-London point of view, the two unpaired p orbitals on each atom forming covalent bonds with its neighbors. The relatively weak interaction between chains is generally agreed to be of the Van der Waals type. Recently, Callen[2] attempted to explain certain optical properties of tellurium by means of a "related" tetragonal crystal structure. Actually, closer inspection of Callen's structure shows that it would produce a metallic conductor, not a semiconductor; hence, the electronic structure of these group VIb substances is still undetermined.

In the following sections, the energy bands of selenium and tellurium are calculated according to the tight-binding scheme in the usual approximation in which only nearest neighbor interactions are taken into account. It is found that there are three well-separated groups of p bands, so that the structure may produce an insulator (or semiconductor) when either two, four, or six p electrons per atom are present. In addition to the band structure, matrix elements for optical transitions between bands have been calculated. Although the "tight-binding model" is somewhat crude, it seems to give essential features of the electronic structure. The optical properties of tellurium as measured by Loferski[3] (absorption edge depending on polarization of incident light) are easily explained by the present calculation.

II. CRYSTAL ORBITALS

In the tight-binding method, the one-electron Bloch functions, $\psi_k(\mathbf{r})$, are constructed as a linear combination

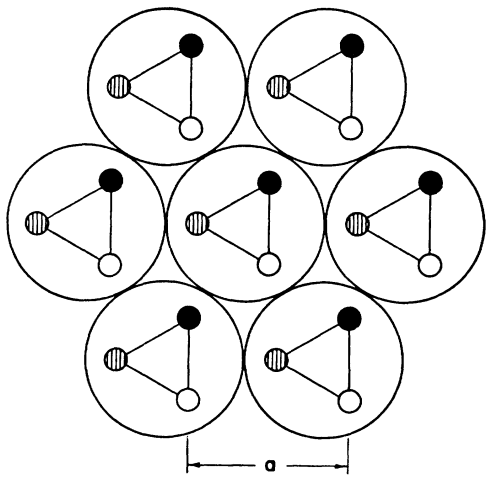

FIG. 1. The crystal structure of selenium and tellurium. Similarly shaded atoms are at the same level in neighboring chains and above each other in the same chain.

* Permanent address: Case Institute of Technology, Cleveland, Ohio.
† National Carbon Company, a Division of Union Carbide and Carbon Corporation.
[1] A. von Hippel, J. Chem. Phys. **16**, 372 (1948).
[2] H. B. Callen, J. Chem. Phys. **22**, 518 (1954).
[3] J. J. Loferski, Phys. Rev. **93**, 707 (1954).

of atomic orbitals:

$$\psi_{\mathbf{k}}(\mathbf{r})=\sum_{n,s,j} B_{ns}\exp(i\mathbf{k}\cdot\mathbf{R}_{js})X_n(\mathbf{r}-\mathbf{R}_{js}), \quad (1)$$

where $X_n(\mathbf{r}-\mathbf{R}_{js})$ is a normalized atomic wave function corresponding to the atomic level n and centered on site $\mathbf{R}_{js}$. The summation over n is over those levels which mix together, s is over the nonequivalent atomic positions in the unit cell, and j is over the unit cells of the crystal. The coefficients B_{ns} may sometimes be determined by symmetry arguments, but usually must be determined by a complete solution to the Schrödinger problem.

Substituting (1) into the Schrödinger equation, we obtain

$$\sum_{n,s,j} B_{ns}\exp(i\mathbf{k}\cdot\mathbf{R}_{js}) \times[-E_{\mathbf{k}}+E_{n0}+W'(\mathbf{r}-\mathbf{R}_{js})]X_n(\mathbf{r}-\mathbf{R}_{js})=0, \quad (2)$$

where

$$W'(\mathbf{r}-\mathbf{R}_{js})=V(\mathbf{r})-W(\mathbf{r}-\mathbf{R}_{js})$$

is the perturbing potential, i.e., $V(\mathbf{r})$ is the crystal potential at $\mathbf{r}$ and $W(\mathbf{r}-\mathbf{R}_{js})$ is the atomic potential at the same point due to the atom at $\mathbf{R}_{js}$. $E_{\mathbf{k}}$ is the energy corresponding to $\mathbf{k}$, and E_{n0} is the energy of the atomic level. If we multiply (2) in turn by the various X_m^* and integrate over all space, we obtain a set of linear equations in the B_{ns}; finally, if we form the determinant of the coefficients of the B_{ns} in these linear equations, and set it equal to zero, we obtain the corresponding secular equation which may be solved for $E_{\mathbf{k}}$.

We shall make the usual tight-binding assumption that two atomic orbitals centered on different atomic sites are orthogonal to each other, i.e.,

$$\int X_m^*(\mathbf{r}-\mathbf{R}_{it})X_n(\mathbf{r}-\mathbf{R}_{js})d\tau=\delta_{mn}\delta_{ij}\delta_{ts}. \quad (3)$$

III. p BANDS

The most important part of the electronic structure are the p bands deriving from the atomic $4p$ levels in selenium, $5p$ levels in tellurium. In order to reduce the problem in complexity, we shall assume that the p levels do not mix with any other type of atomic level. This is probably not the case in the real structure, since the lowest group of p bands very likely mixes with an s level, and the upper group with d states. The mixing of the lowest group is not particularly important to us since these are not the uppermost filled bands in the crystal; more significant is the mixing of p and d levels, which may modify the conduction band of the crystal. We shall see, however, that there is probably either no mixing or mixing with the lowest d band only. Furthermore, we are principally interested in one of the band end points ($\mathbf{k}=0$ or $k_z=\pi/c$) where the band is mostly p or mostly d, even in the mixed case.

There are three nonequivalent atomic sites in the selenium structure, A, B, and C, and three degenerate atomic p levels; hence, the secular equation is of the ninth degree. We recall, however, that the p levels do not mix together in a simple cubic crystal in the nearest neighbor approximation; thus, we anticipate that we can factor the ninth degree secular equation for selenium, for the case where the bond angle in the selenium chain is exactly 90°. As a first approximation, then, we shall work out the band structure of "90°-bonded selenium." This structure is obtained by compressing the crystal slightly along the c axis, the symmetry of the crystal remaining unchanged. Hypothetical selenium (or tellurium) with 90° bonds was first discussed by von Hippel[1] in its relation to the polonium structure.

A set of orthogonal axes, λ, μ, ν is constructed, which because of the 90° bonds may be oriented along the nearest neighbor directions in the selenium chain. The λ direction (see Fig. 3) extends from atom A to C; μ from A to B, and ν from B to C. It will be convenient also to label the set of nearest neighbor distances: $\mathbf{R}_\lambda$, the distance AC in the positive λ directions; $\mathbf{R}_\mu$, etc. It is clear that $\mathbf{R}_\mu+\mathbf{R}_\nu-\mathbf{R}_\lambda=\mathbf{c}$ (the primitive translation vector along the c axis). If we choose our atomic p functions along the directions λ, μ, ν, then the ninth degree secular equation does indeed factor into three identical cubic equations. The nonzero matrix elements (together with their exponential coefficients) are:

$$(p_{\lambda A}|W'|p_{\lambda A})=(p_{\lambda C}|W'|p_{\lambda C})=p_0;$$
$$(p_{\lambda B}|W'|p_{\lambda B})=p_0';$$
$$(p_{\lambda A}|W'|p_{\lambda B})=(p_{\lambda B}|W'|p_{\lambda A})^*=(pp\pi)\exp(i\mathbf{k}\cdot\mathbf{R}_\mu);$$
$$(p_{\lambda B}|W'|p_{\lambda C})=(p_{\lambda C}|W'|p_{\lambda B})^*=(pp\pi)\exp(i\mathbf{k}\cdot\mathbf{R}_\nu);$$
$$(p_{\lambda C}|W'|p_{\lambda A})=(p_{\lambda A}|W'|p_{\lambda C})^*=(pp\sigma)\exp(-i\mathbf{k}\cdot\mathbf{R}_\lambda);$$

with similar matrix elements between $\mu-\mu$, and $\nu-\nu$. Let us abbreviate[4]

$$\epsilon=E_{\mathbf{k}}-E_{p0}-p_0;$$
$$\eta=p_0'-p_0;$$
$$\sigma=(pp\sigma);\quad \pi=(pp\pi).$$

Then, one of the 3×3 secular equations (p_λ) becomes

$$\begin{vmatrix} -\epsilon & \pi\exp(i\mathbf{k}\cdot\mathbf{R}_\mu) & \sigma\exp(i\mathbf{k}\cdot\mathbf{R}_\lambda) \\ \pi\exp(-i\mathbf{k}\cdot\mathbf{R}_\mu) & -\epsilon+\eta & \pi\exp(i\mathbf{k}\cdot\mathbf{R}_\nu) \\ \sigma\exp(-i\mathbf{k}\cdot\mathbf{R}_\lambda) & \pi\exp(-i\mathbf{k}\cdot\mathbf{R}_\nu) & -\epsilon \end{vmatrix}=0, \quad (4)$$

or

$$-\epsilon^2(\epsilon-\eta)+\epsilon(2\pi^2+\sigma^2)-\eta\sigma^2+2\pi^2\sigma\cos k_z c=0. \quad (4a)$$

The three roots of this equation give ϵ as a function of $\mathbf{k}$, and we see that it is only the k_z component that matters. The other two cubic equations obtained from p_μ or p_ν are identical to (4a) so that each of the three roots of (4a) is triply degenerate.

It is instructive to solve (4a) in certain limiting cases. First, assume $(pp\pi)=0$, then the roots are $\epsilon=\eta$, $\pm(pp\sigma)$

[4] In this section π will generally mean the integral $(pp\pi)$; but it has occasionally been necessary to use π in its normal context, i.e., $k_z=\pi/c$.

independent of $\mathbf{k}$. If $(pp\pi)=(pp\sigma)$ and $\eta=0$, then

$$\epsilon=2\sigma\cos(\tfrac{1}{3}k_zc+120°\mathrm{K}) \tag{5}$$

where $K=0, 1, 2$; in this case the two lower bands touch at $\mathbf{k}=0$, and the two upper ones at $k_z=\pi/c$.

Actually the exact solutions of (4a) have a simple analytical form at $\mathbf{k}=0$ and $k_z=\pi/c$. At $\mathbf{k}=0$, the three roots are

$$\epsilon=-\sigma \text{ or } \tfrac{1}{2}\{\sigma+\eta\pm[(\sigma-\eta)^2+8\pi^2]^{\frac{1}{2}}\}; \tag{6}$$

at $k_z=\pi/c$,

$$\epsilon=\sigma \text{ or } -\tfrac{1}{2}\{\sigma-\eta\pm[(\sigma+\eta)^2+8\pi^2]^{\frac{1}{2}}\}. \tag{7}$$

Since $|pp\pi|$ is probably of the order of one-third $(pp\sigma)$, it is feasible to obtain an approximate solution to (4a) in the following compact form (valid for $\eta=0$):

$$\epsilon=\sigma[1+2(\pi/\sigma)^2]^{\frac{1}{2}}\left[\begin{Bmatrix}\pm1\\0\end{Bmatrix}+\begin{Bmatrix}1\\-2\end{Bmatrix}\{1+2(\pi/\sigma)^2\}^{-\frac{3}{2}}(\pi/\sigma)^2\cos k_zc\right], \tag{8}$$

which is plotted in Fig. 2(a). Equation (8) is accurate only to terms in $(\pi/\sigma)^2$. From the usual calculations of two-center integrals, we expect σ and η to be positive, π negative, and $\pi^2<\sigma^2$; in addition, η is probably substantially less than σ. The separation between bands is principally governed by the integral σ, the width of the band by π; the main action of nonzero η is to raise the middle band relative to the other two bands. Even when $\eta\approx\sigma$, the bands do not intersect; an example [obtained by numerical solution of 4(a)] is shown in Fig. 2(b).

Having found the energies ϵ, we may now obtain the coefficients B_{ns} in Eq. (1), and, hence, the relative amplitude of the wave function on the sites A, B, C. At $\mathbf{k}=0$ and $k_z=\pi/c$, the coefficients take on a rather simple form: either (a)

$$B_{\lambda A}:B_{\lambda B}:B_{\lambda C}=-\exp[i\mathbf{k}\cdot(\mathbf{R}_\mu+\mathbf{R}_\nu)]:0:1, \tag{9a}$$

or (b)

$$B_{\lambda A}:B_{\lambda B}:B_{\lambda C}=\exp[i\mathbf{k}\cdot(\mathbf{R}_\mu+\mathbf{R}_\nu)]:H\exp(i\mathbf{k}\cdot\mathbf{R}_\nu):1 \tag{9b}$$

(9a) belongs to the roots $\pm\sigma$; for the other four roots given in (6) and (7), H has one of the following (approximate) values:

$$-\left[\frac{\sigma-\eta}{\pi}+\frac{2\pi}{\sigma-\eta}\right];\quad \frac{2\pi}{\sigma-\eta};\quad -\frac{2\pi}{\sigma+\eta};\quad \left[\frac{\sigma+\eta}{\pi}+\frac{2\pi}{\sigma+\eta}\right].$$

The relative amplitude for the end points of the three bands is shown in Fig. 3 where the amplitude factor includes the Bloch coefficient, $\exp(i\mathbf{k}\cdot\mathbf{R}_{js})$, with $\mathbf{R}_{js}$ measured from the lower C site. The lower band is characterized by a σ bond; at $\mathbf{k}=0$ there is a solitary σ bond between A and C; at $k_z=\pi/c$ the σ bond is weakened slightly (due to normalization) but two small π bonds are gained in the process. The middle band is

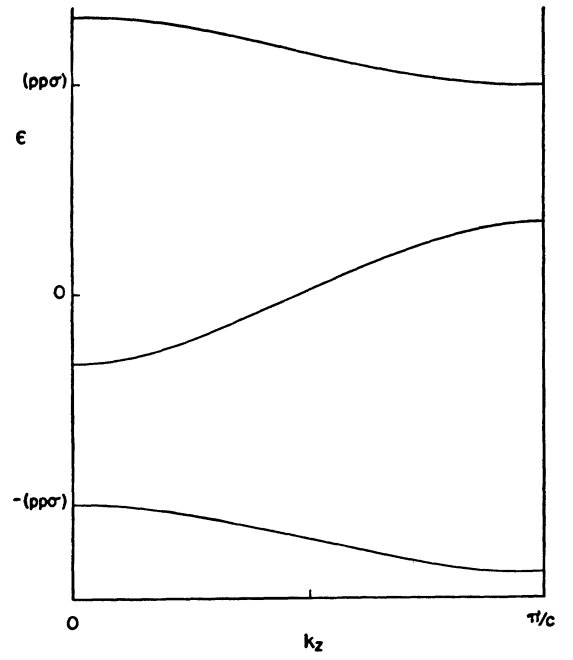

(a)

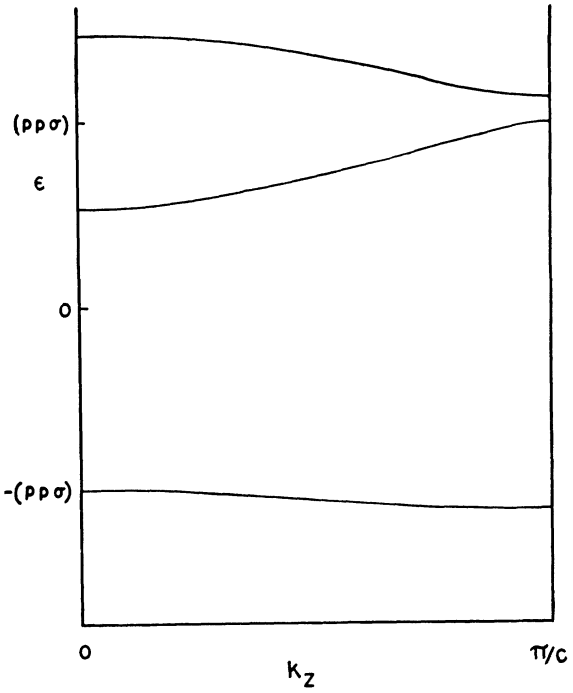

(b)

FIG. 2(a). The p bands of the selenium structure for the particular case of 90° bond angles. $\eta=0$. Each of the bands depicted is triply degenerate. (b) The p bands of the selenium structure for the case of 90° bond angles. $\eta=\sigma$. $|\pi|=\sigma/3$. Each of the bands is triply degenerate.

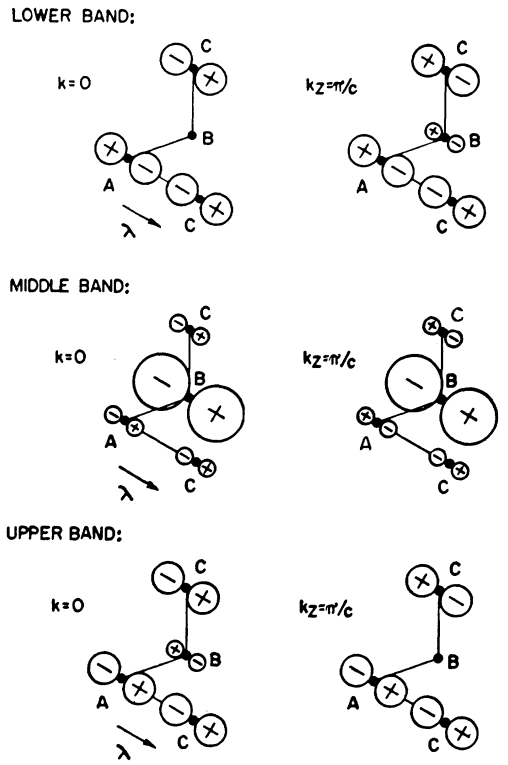

FIG. 3. Schematic drawing showing the relative amplitudes of the atomic orbitals at atomic positions A, B, and C for the end points of the three p_λ bands. The exponential Bloch coefficient is included in the amplitude.

characterized by two π bonds which change to anti-π bonds at $k_z=\pi/c$. The upper band is an antibonding band.

The coefficient ratios, (9a) or (9b), as well as Fig. 3 refer to the p_λ bands. The coefficients of the p_μ and p_ν bands may be obtained from this case by cyclic permutation.

None of the above wave functions, derived solely from p_λ, p_μ, or p_ν has the proper symmetry for the selenium crystal. We may construct wave functions of the proper symmetry, however, as linear combinations of the three degenerate functions. It is evident that for $\mathbf{k}=(0,0,k_z)$ one of these combinations favors the c axis (z direction) of the crystal; we denote this by p_z. The other two may be written as $p_x \pm \sqrt{3} a p_y$, where p_x and p_y favor the x and y axes of the crystal, respectively. a may be determined by symmetry arguments or by the perturbation method outlined in the next section; it is equal to $i/\sqrt{3}$. Now the direction cosines of z, x, and y relative to the λ, μ, ν axes are:

$$\begin{aligned} z&: (-1/\sqrt{3}, 1/\sqrt{3}, 1/\sqrt{3}),\\ x&: (1/\sqrt{2}, 0, 1/\sqrt{2}),\\ y&: (1/\sqrt{6}, 2/\sqrt{6}, -1/\sqrt{6}), \end{aligned} \tag{10a}$$

so that

$$\begin{aligned} p_z &= (1/\sqrt{3})(-p_\lambda + p_\mu + p_\nu),\\ p_x \pm i p_y &= \tfrac{1}{2}[p_\lambda(1\pm a) \pm 2a p_\mu + (1\mp a) p_\nu]. \end{aligned} \tag{10b}$$

The last two combinations will be denoted: p^+ and p^-. Finally, we may write the coefficients of p_z as

$$\begin{aligned} &(B_{\lambda A}:B_{\lambda B}:B_{\lambda C}):(B_{\mu A}:B_{\mu B}:B_{\mu C}):(B_{\nu A}:B_{\nu B}:B_{\nu C})\\ &\quad=(B_{\lambda A}:B_{\lambda B}:B_{\lambda C}):(-B_{\lambda C}:-B_{\lambda A}:-B_{\lambda B}):\\ &\qquad\qquad(-B_{\lambda B}:-B_{\lambda C}:-B_{\lambda A}). \end{aligned} \tag{11}$$

IV. FURTHER SPLITTING OF THE p BANDS

In the selenium crystal with 90° bonds, each of the bands shown in Fig. 2 is triply degenerate, being composed of p_z, p^+, and p^- bands. We can remove the degeneracy, either by adding interactions between more distant neighbors, or by pulling the crystal out along the c axis so as to increase the bond angle. We shall adopt the latter procedure here, since this introduces no new parameters into the theory.

We keep the λ, μ, ν axes fixed in space as we distort the crystal. $\mathbf{R}_\lambda$, $\mathbf{R}_\mu$, and $\mathbf{R}_\nu$ are still the nearest-neighbor distances, but they no longer remain exactly along the directions λ, μ, ν. In fact, if the direction cosines of $\mathbf{R}_\lambda$, $\mathbf{R}_\mu$, and $\mathbf{R}_\nu$ relative to the x, y, z axes are

$$\begin{aligned} R_\mu&: [0, \alpha, (1-\alpha^2)^{\frac{1}{2}}],\\ R_\lambda, R_\nu&: [\tfrac{1}{2}\sqrt{3}\alpha, \pm\tfrac{1}{2}\alpha, \mp(1-\alpha^2)^{\frac{1}{2}}], \end{aligned}$$

and if we define $w=1-\alpha\sqrt{\frac{3}{2}}$, then the direction cosines of $\mathbf{R}_\lambda$, etc., relative to λ, μ, ν are

$$\begin{aligned} \mathbf{R}_\lambda&: (1, -w, -w),\\ \mathbf{R}_\mu&: (-w, 1, w),\\ \mathbf{R}_\nu&: (-w, w, 1), \end{aligned}$$

to first-order terms in w. The matrix elements of the last section are unchanged to first order, but there are

TABLE I. Changes in energy of band end points as the crystal is pulled out along the c axis.

	p_z band	p^+ band	p^- band
Upper group $\mathbf{k}=0$	$2w(\sigma+2\pi)(1-\pi/\sigma)$	$-w(\sigma+2\pi)(1-\pi/\sigma)$	$-w(\sigma+2\pi)(1-\pi/\sigma)$
Upper group $k_z=\pi/c$	$w(\sigma-\pi)$	$w(\sigma-\pi)$	$-2w(\sigma-\pi)$
Middle group $\mathbf{k}=0$	$-4w\pi(1-\pi/\sigma)$	$2w\pi(1-\pi/\sigma)$	$2w\pi(1-\pi/\sigma)$
Middle group $k_z=\pi/c$	$-2w\pi(1-\pi/\sigma)$	$-2w\pi(1-\pi/\sigma)$	$4w\pi(1-\pi/\sigma)$
Lower group $\mathbf{k}=0$	$2w(\sigma-\pi)$	$-w(\sigma-\pi)$	$-w(\sigma-\pi)$
Lower group $k_z=\pi/c$	$w(\sigma+2\pi)(1-\pi/\sigma)$	$w(\sigma+2\pi)(1-\pi/\sigma)$	$-2w(\sigma+2\pi)(1-\pi/\sigma)$

now a number of additional matrix elements:

$$(p_{\lambda A}|W'|p_{\mu B})=(p_{\lambda B}|W'|p_{\mu A})^*=(p_{\mu B}|W'|p_{\lambda A})^*$$
$$=(p_{\mu A}|W'|p_{\lambda B}) \quad =-w(\sigma-\pi)e^{i\mathbf{k}\cdot\mathbf{R}_\mu},$$
$$(p_{\lambda A}|W'|p_{\mu C})=(p_{\lambda C}|W'|p_{\mu A})^*=(p_{\mu C}|W'|p_{\lambda A})^*$$
$$=(p_{\mu A}|W'|p_{\lambda C}) \quad =-w(\sigma-\pi)e^{i\mathbf{k}\cdot\mathbf{R}_\lambda},$$

plus similar elements between $\lambda-\nu$, and $\mu-\nu$. In calculating these matrix elements, Table I from the article by Slater and Koster[5] was found helpful.

For p_z, the set of coefficients (11) must still satisfy each of the simultaneous equations at all $\mathbf{k}=(0,0,k_z)$; at $\mathbf{k}=0$ and $k_z=\pi/c$, (9a) and (9b) are modified slightly to

$$B_{\lambda A}/B_{\lambda B}/B_{\lambda C}=-(1+\Delta)\exp[i\mathbf{k}\cdot(\mathbf{R}_\mu+\mathbf{R}_\nu)]/$$
$$h\exp(i\mathbf{k}\cdot\mathbf{R}_\nu)/1, \quad (12a)$$

$$B_{\lambda A}/B_{\lambda B}/B_{\lambda C}=(1+\Delta)\exp[i\mathbf{k}\cdot(\mathbf{R}_\mu+\mathbf{R}_\nu)]/$$
$$H\exp(i\mathbf{k}\cdot\mathbf{R}_\nu)/1, \quad (12b)$$

where Δ and h are small quantities of the order of w. For p^+ or p^-, the set of coefficients is

$$(B_{\lambda A}:B_{\lambda B}:B_{\lambda C}):(B_{\mu A}:B_{\mu B}:B_{\mu C}):(B_{\nu A}:B_{\nu B}:B_{\nu C})$$
$$=(B_{\lambda A}(1+a):B_{\lambda B}(1+a):B_{\lambda C}(1+a)):$$
$$(2aB_{\lambda C}:2aB_{\lambda A}:2aB_{\lambda B}):$$
$$((1-a)B_{\lambda B}:(1-a)B_{\lambda C}:(1-a)B_{\lambda A}), \quad (13)$$

with (12a) or (12b). But in order that all nine equations be satisfied simultaneously, $a=\pm i/\sqrt{3}$.

The shifts in energy of the end points of the various bands are given in Table I, and the modified p-band structure is shown in Fig. 4. In both selenium and tellurium, w is approximately 0.1.

Adding second neighbor interactions will also remove the degeneracy, but it may reverse the order of some of the bands. Preliminary calculations indicate that some of bands tend to shift in the opposite direction from Table I if the second neighbor $(pp\sigma)_2$ and $(pp\pi)_2$ integrals are large enough and of the same sign as the corresponding first neighbor integrals. But Slater and Koster[5] have shown that when orthogonalized atomic orbitals are used, the second neighbor integrals are often of the opposite sign from expected, and usually are quite small. Further support for the order of the bands as shown in Fig. 4 (at least for tellurium) comes from optical studies of the crystals, as we shall see shortly.

V. d BANDS

There are five atomic d levels and three nonequivalent sites, so that there are fifteen bands. We shall consider only the 90°-bonded crystal here, since even in this case the band structure is almost completely split. With 90° bonds, three of the d levels: $\lambda\mu$, $\mu\nu$, and $\nu\lambda$ do not mix with the other two: $\lambda^2-\mu^2$, $3\nu^2-r^2$. Furthermore, the $\lambda\mu$, $\mu\nu$, and $\nu\lambda$ do not mix with each other in the nearest neighbor approximation. Hence, the secular equation factors into three identical cubics and a 6×6 equation. The cubic equation is similar to the p-band cubic with ϵ'' replacing ϵ, $\eta\approx0$, and with $(dd\delta)$ and $(dd\pi)$ replacing $(pp\sigma)$ and $(pp\pi)$ respectively. Since $(dd\delta)$ is of the opposite sign to $(pp\sigma)$, the bands will slant in the opposite direction (see the dotted curves in Fig. 5).

The $\lambda^2-\mu^2$ and $3\nu^2-r^2$ levels mix together to form a sixth degree secular equation. This equation involves the integrals $(dd\sigma)$, hence will give rise to the lowest of the d bands. We may easily construct the secular determinant by using Table I of reference 5; abbreviating $\sigma=(dd\sigma)$, $\delta=(dd\delta)$, we obtain

$$\begin{vmatrix}
-\epsilon'+\frac{1}{4}\eta' & \frac{1}{4}(3\sigma+\delta)e^{i\mathbf{k}\cdot\mathbf{R}_\mu} & \frac{1}{4}(3\sigma+\delta)e^{i\mathbf{k}\cdot\mathbf{R}_\lambda} & 0 & \frac{1}{4}\sqrt{3}(\sigma-\delta)e^{i\mathbf{k}\cdot\mathbf{R}_\mu} & -\frac{1}{4}\sqrt{3}(\sigma-\delta)e^{i\mathbf{k}\cdot\mathbf{R}_\lambda} \\
 & -\epsilon'+\eta' & \delta e^{i\mathbf{k}\cdot\mathbf{R}_\nu} & \frac{1}{4}\sqrt{3}(\sigma-\delta)e^{-i\mathbf{k}\cdot\mathbf{R}_\mu} & 0 & 0 \\
\text{(complex} & & -\epsilon'+\eta' & -\frac{1}{4}\sqrt{3}(\sigma-\delta)e^{-i\mathbf{k}\cdot\mathbf{R}_\lambda} & 0 & 0 \\
\text{conjugate)} & & & -\epsilon'+\frac{3}{4}\eta' & \frac{1}{4}(\sigma+3\delta)e^{i\mathbf{k}\cdot\mathbf{R}_\mu} & \frac{1}{4}(\sigma+3\delta)e^{i\mathbf{k}\cdot\mathbf{R}_\lambda} \\
 & & & & -\epsilon' & \sigma e^{i\mathbf{k}\cdot\mathbf{R}_\nu} \\
 & & & & & -\epsilon'
\end{vmatrix},$$

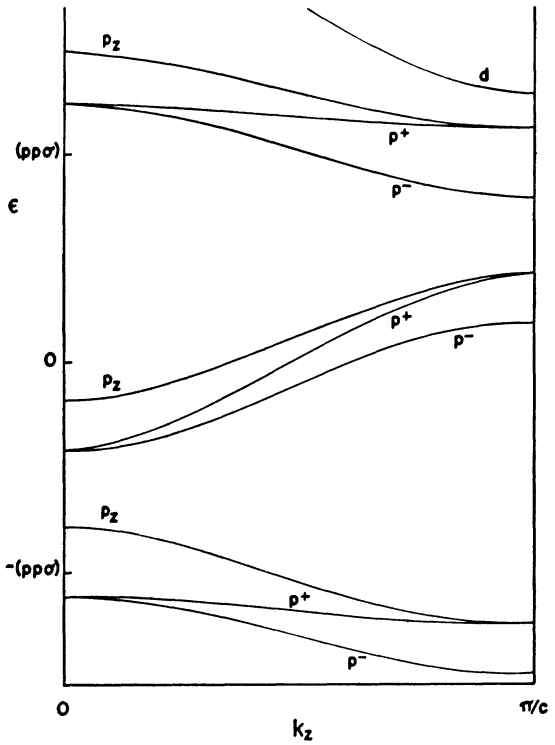

FIG. 4. The nine p bands of the selenium structure for the case where the bond angles are greater than 90°. The lowest d band is also shown, but its exact position relative to the p bands has not been calculated.

[5] J. C. Slater and G. F. Koster, Phys. Rev. **94**, 1498 (1954).

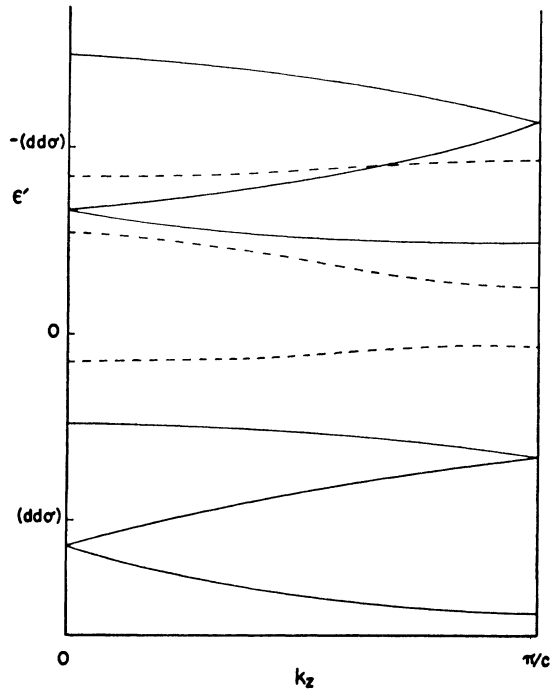

FIG. 5. The fifteen d bands of the selenium structure for the particular case of 90° bond angles. The three broken curves are each triply degenerate.

which must be set equal to zero. Here

$$\epsilon' = E_{\mathbf{k}} - E_{d0} - d_0;$$
$$\eta' = d_0' - d_0;$$

where

$$d_0 = (d_{3\nu^2-r^2,B} | W' | d_{3\nu^2-r^2,B});$$
$$d_0' = (d_{\lambda^2-\mu^2,B} | W' | d_{\lambda^2-\mu^2,B}).$$

Now, $\lambda^2-\mu^2$ and $3\nu^2-r^2$ favor the ν direction, which is not a symmetry direction in the crystal. For $\mathbf{k}$ oriented along the c axis of the crystal, the correct wave function should favor the z direction. Such a function may be constructed as

$$(3\nu^2-r^2)_A + (3\lambda^2-r^2)_B + (3\mu^2-r^2)_C + g\{(\lambda^2-\mu^2)_A + (\mu^2-\nu^2)_B + (\nu^2-\lambda^2)_C\},$$

where g is a constant to be determined. This construction is facilitated by the fact that $3\lambda^2-r^2$, $3\mu^2-r^2$, etc., may be obtained as linear combinations of the two normalized functions: $3\nu^2-r^2$ and $\lambda^2-\mu^2$. Thus,

$$3\lambda^2-r^2 = -\tfrac{1}{2}(3\nu^2-r^2) + \tfrac{1}{2}\sqrt{3}(\lambda^2-\mu^2),$$

etc. The coefficient ratio of the six linear equations becomes

$$(B_{\lambda^2-\mu^2,A} : B_{\lambda^2-\mu^2,B} : B_{\lambda^2-\mu^2,C}) : (B_{3\nu^2-r^2,A} : B_{3\nu^2-r^2,B} : B_{3\nu^2-r^2,C})$$
$$= (g : \tfrac{1}{2}(\sqrt{3}-g) : -\tfrac{1}{2}(\sqrt{3}+g)) : (1 : -\tfrac{1}{2}(1+\sqrt{3}g) : -\tfrac{1}{2}(1-\sqrt{3}g)). \quad (14)$$

This set of coefficients does indeed satisfy each of the six linear equations, but only for the case $\eta'=0$. This case gives us all of the essential features of the d-band structure; hence we limit ourselves by this restriction. We find that g is purely imaginary:

$$g = -(2i/\sqrt{3})[(\sigma-\delta)/(\sigma+\delta)] \cot(\tfrac{1}{3}k_z c) \pm i\{1+(4/3)[(\sigma-\delta)^2/(\sigma+\delta)^2] \cot^2(\tfrac{1}{3}k_z c)\}^{\frac{1}{2}}, \quad (15)$$

and

$$\epsilon' = -\tfrac{1}{2}(\sigma+\delta) \cos(\tfrac{1}{3}k_z c)\{1 \pm 2[(\sigma-\delta)^2/(\sigma+\delta)^2 + \tfrac{3}{4} \tan^2(\tfrac{1}{3}k_z c)]^{\frac{1}{2}}\}. \quad (16)$$

The second set of coefficients is obtained from (14) by multiplying the B and C amplitudes by ω and ω^2, respectively, where $\omega = (1)^{\frac{1}{3}} = e^{2\pi i/3}$. The third set: B and C amplitudes multiplied by ω^2 and ω, respectively. The four other roots of the secular equation are obtained from (16) by replacing $\frac{1}{3}k_z c$ by $\frac{2}{3}\pi \pm \frac{1}{3}k_z c$. All fifteen d bands are shown in Fig. 5.

VI. OPTICAL TRANSITIONS

In selenium and tellurium, the lower and middle group of p bands are filled, the upper p group and the d bands are empty. Optical transitions correspond to transitions between the middle p group and one of the conduction bands. If the bands are ordered as in Fig. 4, then the long wavelength limit corresponds to a $p \rightarrow p$ transition at $k_z = \pi/c$. It is possible, since we do not know the exact values of p_0 and d_0, that the lowest d band actually cuts across the upper p group. Then, the absorption limit would correspond to $p \rightarrow d$, still at $k_z = \pi/c$. In this case there would be mixing between the p and d levels, and the simple theory of the preceding sections would not be strictly true; nevertheless, the lowest part of the "d band" would still be predominantly d.

Matrix elements for the optical transitions are rather easy to work out in the tight-binding approximation provided the number of interacting neighbors is not very large. We are interested in the matrix element:

$$(\psi_{\mathbf{k}'f}^* | e^{i\mathbf{q}\cdot\mathbf{r}} \boldsymbol{\epsilon}_0 \cdot \nabla | \psi_{\mathbf{k}i}),$$

where $\psi_{\mathbf{k}i}$ and $\psi_{\mathbf{k}'f}$ are wave functions of the form (1) for the particular electron which changes its state during the absorption, $\mathbf{q}$ is the wave number of the incident radiation, and $\boldsymbol{\epsilon}_0$ is a unit vector along the polarization direction of the electric vector in the radiation. Since the wavelength of the radiation is very large compared to interatomic distances, and since $\mathbf{k}' = \mathbf{k}+\mathbf{q} \approx \mathbf{k}$ in the one-electron scheme, substantial simplifications may be made in the form of the matrix element. Further, the matrix element of $\boldsymbol{\epsilon}_0 \cdot \nabla$ may be converted in the usual way to one of ξ, where ξ is the magnitude of an arbitrary

vector in the direction of polarization, ε_0:

$$\text{M.E.} \propto \sum_{t,s,j,m,n} B_{mt}^*(\mathbf{k}) B_{ns}(\mathbf{k}) e^{i\mathbf{k}\cdot(\mathbf{R}_{js}-\mathbf{R}_t)} \times \int X_{fm}^*(\mathbf{r}-\mathbf{R}_t)\xi X_{in}(\mathbf{r}-\mathbf{R}_{js})d\tau, \quad (17)$$

where s, j, n refer to the initial state and are as per Eq. (1), m is an index to summed over levels contributing to the final one-electron function, and t is summed over to all atoms interacting with a given s, j. Finally ξ is written as

$$\xi = d_1\lambda + d_2\mu + d_3\nu, \quad (18)$$

where d_1, d_2, and d_3 are the direction cosines of the polarization direction with respect to λ, μ, ν axes. When only dominant interactions are considered, the number of nonzero terms retained in (17) is not particularly large. The summation over j may be replaced by N, where N is the number of unit cells in the crystal.

We first consider $p \rightarrow d$ transitions since they are simpler. Here the dominant contributions come from terms in which the two atomic orbitals are on the same atom. The quantities, $(\lambda^2-\mu^2, A\,|\lambda|\,\lambda, A)$, etc., are well-known atomic matrix elements. Neglecting all but the dominant contributions, (17) becomes

$$\text{M.E.} \propto (15)^{-\frac{1}{2}} \sum_s [B^*_{3\nu^2-r^2,s}(2d_3 B_{\nu,s} - d_1 B_{\lambda,s} - d_2 B_{\mu,s}) + \sqrt{3} B^*_{\lambda^2-\mu^2,s}(d_1 B_{\lambda,s} - d_2 B_{\mu,s})]. \quad (19)$$

Now the lowest d band has the coefficients:

$$(B_{\lambda^2-\mu^2,A} : B_{\lambda^2-\mu^2,B} : \cdots : B_{3\nu^2-r^2,C}) = (g : \tfrac{1}{2}(\sqrt{3}-g)\omega : \tfrac{1}{2}(\sqrt{3}+g)\omega^2) : (1 : -\tfrac{1}{2}(1+\sqrt{3}g)\omega : -\tfrac{1}{2}(1-\sqrt{3}g)\omega^2); \quad (20)$$

using these together with (11), we find

$$\text{M.E.}_{p_z \rightarrow d} \propto (15)^{-\frac{1}{2}}(d_3 - \omega^2 d_1 + \omega d_2) \times [2B_{\lambda B} - \omega B_{\lambda A} - \omega^2 B_{\lambda C} + \sqrt{3} g(\omega B_{\lambda A} - \omega^2 B_{\lambda C})]. \quad (21)$$

This vanishes if the radiation is polarized in the z direction [refer to (10a)]. Actually the quantity in square brackets vanishes right at $k_z = \pi/c$; at slightly smaller values of k_z, however, the matrix element vanishes only if the light is polarized along the c axis of the crystal.

Using (20) together with (13), we are able to calculate the matrix elements for $p^+ \rightarrow d$ and $p^- \rightarrow d$. The former again vanishes if the radiation is polarized along the c axis; the latter vanishes for polarization perpendicular to the c axis. Hence, there are two absorption edges. From the ordering of p bands as given in Fig. 4, it is evident that the absorption edge for light polarized perpendicular to the c axis is at the longer wavelength. This is in agreement with the measurements on tellurium as reported by Loferski.[3]

For $p \rightarrow p$ transitions, the contribution from terms in which the atomic orbitals are on the same atom vanishes; hence, we must consider interactions between atomic orbitals on nearest neighbors. The elemental matrix elements are either zero or of the following two types, which we denote by O_1 and O_2:

$$(\lambda, A\,|\,\nu\,|\,\nu, C) = O_1, \qquad (\nu, B\,|\,\nu\,|\,\nu, C) = O_2. \quad (22)$$

Hence, the matrix element, (17), becomes

$$\begin{aligned}\text{M.E.} \propto\ & d_3 O_2 [B^*_{f\nu B} B_{\nu C} e^{i\mathbf{k}\cdot\mathbf{R}_\nu} - B^*_{f\nu C} B_{\nu B} e^{-i\mathbf{k}\cdot\mathbf{R}_\nu}] \\ & + d_3 O_1 [B^*_{f\nu A} B_{\nu C} e^{i\mathbf{k}\cdot\mathbf{R}_\lambda} - B^*_{f\lambda C} B_{\nu A} e^{-i\mathbf{k}\cdot\mathbf{R}_\lambda} \\ & + B^*_{f\nu A} B_{\lambda C} e^{i\mathbf{k}\cdot\mathbf{R}_\lambda} - B^*_{f\nu C} B_{\lambda A} e^{-i\mathbf{k}\cdot\mathbf{R}_\lambda} \\ & + B^*_{f\mu A} B_{\nu B} e^{i\mathbf{k}\cdot\mathbf{R}_\mu} - B^*_{f\mu B} B_{\nu A} e^{-i\mathbf{k}\cdot\mathbf{R}_\mu} \\ & + B^*_{f\nu A} B_{\mu B} e^{i\mathbf{k}\cdot\mathbf{R}_\mu} - B^*_{f\nu B} B_{\mu A} e^{-i\mathbf{k}\cdot\mathbf{R}_\mu}] \\ & + \cdots, \end{aligned} \quad (23)$$

plus similar terms in d_1 and d_2. The subscript f refers to the final state. For $p_z \rightarrow p_z$ at $\mathbf{k} = (0,0,\pi/c)$, we find with the aid of (11)

$$\text{M.E.}_{p_z \rightarrow p_z} \propto -(d_1 - d_2 - d_3) i\sqrt{3} O_1 H, \quad (24)$$

where H is the symbol in (9b) referring to the end point of the middle band, namely, $H = [(\sigma+\eta)/\pi + 2\pi/(\sigma+\eta)]$. Equation (24) vanishes if the radiation is polarized perpendicular to the c axis (z direction) of the crystal.

In a similar fashion, we find that the matrix element for $p^- \rightarrow p^-$ vanishes for the same polarization, but $p_z \rightarrow p^-$ and $p^+ \rightarrow p^-$ vanish if the polarization direction is parallel to the c axis. Referring to Fig. 4, we find two absorption edges corresponding to transitions from the middle two p levels to the lowest of the upper p group at $k_z = \pi/c$. Again, the absorption edge for light polarized perpendicular to the c axis is at the longer wavelength.

Thus, we cannot distinguish between $p \rightarrow d$ and $p \rightarrow p$ on the basis of this single criterion. It is probable, however, that a detailed analysis of the absorption beyond the edge could distinguish between these two cases, since the behavior of (21) and (24) are quite different in the vicinity of $k_z = \pi/c$. At all events, the structure of the lowest conduction band is really not much different in the two cases: where the lowest d band does or does not cut the upper p group.

VII. EFFECT OF HYDROSTATIC PRESSURE

Bridgman[6] has measured the compressibility of tellurium under hydrostatic pressure, finding an anomalous *expansion* parallel to the c axis and a normal contraction perpendicular to this axis. Hence, it appears that one of the effects of hydrostatic pressure on Te is to increase the bond angle between adjacent bonds in each chain. Bridgman[7] also observed a decrease in resistivity of tellurium under hydrostatic pressure, the decrease being more than a factor of 600 at a pressure of 30 000 kg/cm^2, and from the decrease Bardeen[8] was able to calculate the

[6] P. W. Bridgman, Proc. Am. Acad. Arts Sci. **60**, 303 (1925).
[7] P. W. Bridgman, Proc. Am. Acad. Arts Sci. **72**, 159 (1938).
[8] J. Bardeen, Phys. Rev. **75**, 1777 (1949).

corresponding reduction in energy gap between valence and conduction bands ($E_g \approx 0$ at pressure of 30 000 kg/cm^2).

If we assume that the principal effect of hydrostatic pressure is the effect on the bond angles mentioned above, then we find that for $p \rightarrow p$ transitions the energy gap *decreases*, in agreement with experiment. In fact, according to Table I the change in energy gap for this case is

$$\Delta E_g = -2(\Delta w)(\sigma - 2\pi + \pi^2/\sigma), \quad (25)$$

where Δw is the change in the quantity, w, defined in Sec. IV.

For $p \rightarrow d$ transitions, we cannot predict with certainty that the energy gap decreases with increasing w, since the d bands (Fig. 5) have only been calculated for the 90° bonded crystal.

VIII. CONCLUSION

The tight-binding scheme has been applied to the selenium structure and appears to give the essential features of the electronic structure. It appears that the scheme may be used to advantage in obtaining first approximations to the band structure of certain other complicated crystalline materials. Matrix elements for optical transitions are fairly easy to work out in the tight-binding approximation provided the dominant "atomic" interactions are sufficient for one's purpose. Application to tellurium has explained the polarization-dependent absorption edge observed by Loferski.[3]

PHYSICAL REVIEW VOLUME 105, NUMBER 4 FEBRUARY 15, 1957

Incoherent Neutron Scattering by Polycrystals

G. PLACZEK*
Institute for Advanced Study, Princeton, New Jersey
(Received November 16, 1956)

General expressions are given for the first terms in the expansion in powers of the neutron to nuclear mass ratio of the total cross section for incoherent scattering of neutrons by polycrystals. Special limiting cases of these expressions had been published earlier.

A NEW method of calculation for the total cross section of incoherent scattering of slow neutrons by a polycrystal was presented very briefly in an earlier publication and a few results were mentioned for the special case of low neutron energy and high crystal temperature.[1] The aim of the present note is to give the main equations of the method for the general case. Regarding the crystal the simplifying assumption is made that it has a Bravais lattice and that all lattice vibrations (phonons) have the same velocity, irrespective of wave vector and direction of polarization.

We denote by x and y the energies of incident and scattered neutrons, expressed in units of the Debye temperature θ_D of the crystal. In the same units, T is the crystal temperature and ξ the energy of a phonon. The mass M of the nuclei in the crystal, in units of the neutron mass, is the expansion parameter of the method: the total cross section is expanded in powers of M^{-1}. All cross sections are given in units of the bound incoherent nuclear cross section previously denoted by s.[1] Finally the quantity F, a function of the temperature, is defined by

$$F = \tfrac{1}{2}\int_0^1 \coth(\xi/2T)\xi d\xi.$$

It is the mean square deviation of a nucleus in the crystal from its equilibrium position, in units of the de Broglie wavelength of a nucleus with energy θ_D.

Decomposing the total scattering cross section σ into cross sections σ_l for processes in which l phonons are emitted or absorbed, one has

$$\sigma = \sum_{l=0}^{\infty} \sigma_l, \quad (1)$$

where[2]

$$\sigma_l = \int_{-1}^{1}\int_{-1}^{1}\cdots\int_{-1}^{1} \prod_{i=1}^{l}\left[\coth\left(\frac{\xi_i}{2T}\right) - 1\right]\xi_i d\xi_i \times \psi_l\left(x, x + \sum_{i=1}^{l}\xi_i\right), \quad (2)$$

* The present note contains results obtained by George Placzek a few years ago and never published, except in very fragmentary form as a Letter to the Editor [G. Placzek, Phys. Rev. **93**, 895 (1954)]. In view of the importance of these results for actual computation of slow-neutron scattering cross sections, it was considered useful to publish them after Dr. Placzek's death, as a complement to the above-mentioned letter. The author's original notes have been reviewed and edited for publication by L. Van Hove, Utrecht, Netherlands.

[1] G. Placzek, Phys. Rev. **93**, 895 (1954).

[2] G. L. Squires, Proc. Roy. Soc. (London) **A212**, 192 (1952). The equations of this paper must be rearranged and expressed with the present notation to reduce to the more compact form (2).